

A 2'-O-Methyltransferase Responsible for Transfer RNA Anticodon Modification Is Pivotal for Resistance to *Pseudomonas syringae* DC3000 in *Arabidopsis*

Vicente Ramírez,¹ Beatriz González,¹ Ana López,^{1,2} Maria Jose Castelló,¹ Maria José Gil,¹ Bo Zheng,³ Peng Chen,⁴ and Pablo Vera^{1,†}

¹Instituto de Biología Molecular y Celular de Plantas, Universidad Politécnica de Valencia-C.S.I.C, Ciudad Politécnica de la Innovación, Edificio 8E, Valencia, Spain; ²Institute for Translational Plant and Soil Biology, Department of Animal and Plant Sciences, The University of Sheffield, Sheffield, U.K.; ³College of Horticulture and Forestry Sciences, Huazhong Agricultural University, Wuhan, China; and ⁴National Key Laboratory of Crop Genetic Improvement and National Centre of Plant Gene Research, HuaZhong Agricultural University, Wuhan, China

Accepted 2 July 2018.

Transfer RNA (tRNA) is the most highly modified class of RNA species in all living organisms. Recent discoveries have revealed unprecedented complexity in the tRNA chemical structures, modification patterns, regulation, and function, suggesting that each modified nucleoside in tRNA may have its own specific function. However, in plants, our knowledge of the role of individual tRNA modifications and how they are regulated is very limited. In a genetic screen designed to identify factors regulating disease resistance in *Arabidopsis*, we identified *SUPPRESSOR OF CSB3 9 (SCS9)*. Our results reveal *SCS9* encodes a tRNA methyltransferase that mediates the 2'-O-ribose methylation of selected tRNA species in the anticodon loop. These *SCS9*-mediated tRNA modifications enhance susceptibility during infection with the virulent bacterial pathogen *Pseudomonas syringae* DC3000. Lack of such tRNA modification, as observed in *scs9* mutants, specifically dampens plant resistance against DC3000 without compromising the activation of the salicylic acid signaling pathway or the resistance to other biotrophic pathogens. Our results support a model that gives importance to the control of certain tRNA modifications for mounting an effective disease resistance in *Arabidopsis* toward DC3000 and, therefore, expands the repertoire of molecular components essential for an efficient disease resistance response.

Transfer RNAs (tRNAs) are noncoding RNAs responsible for the addition of amino acids to the C-terminus of translating proteins. These molecules are 75 to 78 nucleotides long, with a characteristic three-dimensional L-shape, usually represented

Vicente Ramírez and Beatriz González contributed equally to this work.

[†]Corresponding author: Pablo Vera; E-mail: vera@ibmcp.upv.es

Funding: Funding for this work were supported by Generalitat Valenciana, grant Prometeo2014/024 and MINECO, grant BFU2015-68199-R.

*The e-Xtra logo stands for “electronic extra” and indicates that seven supplementary figures and three supplementary tables are published online.

This article is in the public domain and not copyrightable. It may be freely reprinted with customary crediting of the source. The American Phytopathological Society, 2018.

in the form of a cloverleaf displaying the four distinctive stem-loop arms, the acceptor arm, the variable D arm, the anticodon arm, and the variable/TΨC arm, which are generated by internal base pairing. A distinctive feature of tRNA is that, among the 107 posttranscriptional modifications found in RNA, 92 of these modified nucleosides are present on tRNA molecules that are involved in the mature tRNA processing required for its function (Machnicka et al. 2013). Interestingly, the biosynthetic pathway of the majority of tRNA modifications include at least a methylation step, and the number of modified bases varies among individual tRNA types and among different prokaryote and eukaryote species (Machnicka et al. 2014). Modifications vary from a single methylation on the ribose to more complicated modifications at different positions on the purine or pyrimidine ring (El Yacoubi et al. 2012; Hori 2014; Machnicka et al. 2013). Comprehensive information on structures and positions of these modifications in tRNA molecules, tRNA biosynthetic pathways, and responsible enzymes are deposited in different RNA modification databases (e.g., the MODOMICS database). Nucleoside tRNA modifications remain extensively studied in bacteria and yeast, and data has most recently been reported in humans. The fact that posttranscriptional modifications are highly conserved, based on the variety of organisms reported, underscores their importance. In bacteria and *Saccharomyces cerevisiae*, the relationship between the type of modification in tRNAs and metabolism has been suggested as a regulatory device acting as biological sensors, continually adjusting based on growth conditions (El Yacoubi et al. 2012; Novoa et al. 2012; Phizicky and Hopper 2010). However, little is documented on tRNA-modified nucleosides in plants, and research in genetic and biochemical regulation is still in its infancy. However, a recent study performed in *Arabidopsis* and hybrid aspen (*Populus tremula* × *tremuloides*) identified 21 modified nucleosides in tRNAs in both species (Chen et al. 2010). In addition, very few plant tRNA sequences are available to identify modified nucleosides on different positions of individual tRNA species, and information on plant tRNA modifying enzymes and the genetic characterization of mutant strains defective in specific tRNA modifications is still scant (Burgess et al. 2015; Chen et al. 2010; David et al. 2017; Kalhor and Clarke 2003; Miyawaki et al. 2006; Walden et al. 1982; Wang et al. 2017; Zhou et al. 2013).

From a compilation of tRNA sequences, Jühling et al. (2009) estimated that the cytoplasmic tRNAs of *S. cerevisiae* contain, on average, 12.6 modifications per tRNA molecule and,

in particular, 2.6 of these modifications occur within the anticodon loop (N₃₂-N₃₈). The rest of the modifications occur in the main body of the tRNA and appear crucial for folding and stability of the molecule, with the absence of certain body modifications eliciting a quality control pathway that results in the degradation of specific tRNAs at different stages of biosynthesis (Thompson and Parker 2009). Instead, many tRNA modifications that occur in the anticodon loop play several crucial roles in translation; deficiencies in modified nucleosides, like those influencing decoding of certain codons, lead to reduced translation efficiency and increased errors, ultimately affecting gene expression and cell metabolism (Agris et al. 2007; Björk 1995; Chan et al. 2012; Chen et al. 2010; Dedon and Begley 2014; Gu et al. 2014; Phizicky and Hopper 2010). As proposed by Chan et al. (2010, 2012), in response to external cues, nucleoside modification changes may be used as a “regulatory module” to timely adapt the cell to environmental changes in a fast, broad, and effective manner. In the majority of cases, however, it remains unclear exactly which tRNAs are specifically affected by a lack of specific modification and how the absence of specific tRNA modifications conferred specific phenotypes. One such crucial modification of a tRNA is the concurrent 2'-*O*-methylation of N32 and N34. The latter occupies the anticodon wobble nucleotide, which forms Nm32 and Nm34 in the anticodon loop. In yeast, 2'-*O*-methylation occurs on C32 and N34 of tRNA^{Phe}, tRNA^{Leu}, and tRNA^{Trp}, and such covalent modifications are mediated by the methyltransferase (MTase) Trm7p (Guy et al. 2012; Pintard et al. 2002); interestingly *trm7* mutant strains show growth reduction, presumably due to translation defects (Pintard et al. 2002). These 2'-*O*-methylations of the anticodon loop are highly conserved in eukaryotes and, in humans, defects in such modifications are associated with mental disorders (Kirchner and Ignatova 2015; Kuchino et al. 1982; Takano et al. 2008). Despite these observations in yeast and humans, no evidence exists, to date, supporting the importance of this tRNA modification type in plants and the consequences of a failure in its control by TRM7 homologous genes (Burgess et al. 2016).

The present study provides insights into the functional implications that some specific tRNA modifications at the anticodon loop had on the activation of an efficient disease-resistance response in *Arabidopsis* toward the bacterial pathogen *Pseudomonas syringae* DC3000 (DC3000), the causal agent of bacterial speck disease. During a search for genetic suppressors in *Arabidopsis* for the enhanced disease-resistance *csb3* mutant (Gil et al. 2005), we identified the *SCS9* gene (standing for suppressor of *csb3*) encoding a functional homolog of the yeast MTase Trm7p. Our results provide evidence that *SCS9* is crucial to maintain intact plant resistance toward DC3000. We employed genetic, molecular, and physiological analyses, and concluded it is vital to maintain an intact 2'-*O*-methylation of the tRNA anticodon loop molecules to ensure plant resistance against DC3000. Therefore, our results uncover a new critical component required for disease resistance in *Arabidopsis*.

RESULTS

scs9 identification.

The *csb3 Arabidopsis*-enhanced disease-resistant mutant was isolated during a search for negative disease-resistance regulators to biotrophic pathogens (Gil et al. 2005). Enhanced disease resistance to DC3000 occurred in *csb3* plants, with increased accumulation of salicylic acid (SA) and constitutive expression of pathogenesis-related (*PR*) genes. Moreover, epistasis analysis with different genes involved in the SA signal transduction pathway revealed *csb3* plants required intact SA

synthesis and its recognition through the NPR1 receptor (Gil et al. 2005).

We conducted a screen for *csb3* suppressors in a second-site mutagenesis to further our understanding of plant immunity. Hence, homozygous *csb3* seeds were mutagenized with ethyl methanesulfonate (EMS), and approximately 20,000 M2 seeds were grown and screened to identify individuals that no longer exhibited enhanced resistance to DC3000 attributable to the *csb3* mutation. This screen rendered the isolation of the recessive *scs9* (standing for suppressors of *csb3*) mutant (Fig. 1). *csb3 scs9* plants lost the distinguishable morphological and growth-arrest phenotype of *csb3* plants (Fig. 1A). The *scs9* mutant, when segregated from *csb3*, retained only a partial retardation in growth when compared with full-grown Col-0 plants (Fig. 1D). Such retardation in growth in the mutant could be observed from early stages of seedling development and accounted for a 20% reduction in fresh weight when compared with Col-0 (Supplementary Fig. S1). Also, the pathogen-responsive marker *pP69C::GUS* gene (Jordá and Vera 2000), constitutively expressed in the single *csb3* mutant (Gil et al. 2005), was abrogated in the double *csb3 scs9* mutant (Fig. 1B). Moreover, comparative observations of DC3000 growth rates in Col-0, *csb3*, and *csb3 scs9* infected leaves showed the *scs9* mutation blocks the characteristic enhanced resistance to DC3000 due to the *csb3* mutation (Fig. 1C). Notably, *csb3 scs9* plants were far more susceptible to DC3000 than Col-0 plants, and the observed enhanced susceptibility was of a similar magnitude, if not higher, to that observed in *npr1* plants (Fig. 1C). Furthermore, genetic analyses indicated the *scs9* mutation was extragenic to *csb3* and, when segregated from the *csb3* mutant background by backcrossing to Col-0 plants, the compromised immune response conferred by the *scs9* mutation alone was maintained in the absence of the *csb3* mutation (Fig. 1C). The enhanced bacterial growth in the single *scs9* mutant was accompanied by distinguishable symptoms of induced chlorosis, presumably due to high levels of bacterial growth reached in the mutant (Fig. 1D). Interestingly, infection with the bacterial mutant strain *HrpC*, affected in the type III secretion system (Deng et al. 1998), revealed no enhanced susceptibility in *scs9* plants compared with Col-0 (Fig. 1E), while the *nhol Arabidopsis* mutant, here used as a control for nonhost resistance, supported a 100-fold enhancement in bacterial growth (Fig. 1E). This observation suggested the enhanced susceptibility of *scs9* plants to DC3000 is host-specific and dependent on bacterial effectors. Potential changes in the susceptibility of *scs9* plants to biotrophic pathogens were further investigated by inoculating plants with a virulent strain (WACO9) of the obligate oomycete *Hyaloperonospora arabidopsidis*. Disease severity was assessed at 7 days postinoculation in lactophenol trypan blue-stained leaves. The leaves were classified into four categories (I to IV) according to their degree of colonization by the oomycete (Fig. 1F; Supplementary Table S1). Both, Col-0 and *scs9* plants exhibited a similar degree of colonization by the oomycete and showed no significant differences. This result indicates that *SCS9* is not required for the immune response toward *H. arabidopsidis* and further substantiates its value in establishing an effective and specific immune response toward DC3000. In summary, these results point toward *SCS9* as an important locus regulating plant resistance to DC3000 in *Arabidopsis*.

scs9 plants retain intact components of innate and SA-mediated immunity.

The enhanced disease susceptibility of *scs9* plants toward DC3000 might result from a lack of pathogen recognition or defects at any step downstream in the signaling pathway leading to activation of plant immune responses. Insights into

the level at which *scs9* might be operating were gained by studying major hallmarks of plant immune responses in search of defects that might explain the compromised mutant immunity. We first tested whether *scs9* plants might be affected in early recognition of pathogen-associated molecular patterns (PAMPs) by measuring PAMP-mediated deposition of the β -1,3-glucan cell-wall polymer callose. The degree of callose deposition induction in PAMP-treated leaves was monitored after staining with aniline blue, was examined by UV fluorescence microscopy (Fig. 2A), and was quantified by counting yellow pixels on digital images (Fig. 2B). The response to the bacterial flagellar peptide elicitor flg22 or to chitosan, which are unrelated PAMPs that induce callose deposition in *Arabidopsis*, was similar in *scs9* and Col-0 seedlings (Fig. 2A and B). *MYB51* gene expression (Clay et al. 2009) and mitogen-activated protein kinase (MAPK) activation (Asai et al. 2002; Bethke et al. 2009) constitute additional hallmarks for early PAMP-mediated immune signaling. Induction of *MYB51* transcript accumulation, measured by reverse transcription-quantitative polymerase chain reaction (RT-qPCR) at 5, 10, and 60 min after flg22 application, revealed no differences between Col-0 and *scs9* plants (Fig. 2C). Early elicitation of MAPK activation following flg22 application was visualized by employing an antibody that recognized the phosphorylated residues within the MAPK activation loop. Western blot analysis of protein extracts derived from Col-0 and *scs9* plants revealed positive immunoreactive signals in the two polypeptides corresponding to MPK6 and MPK3 (Fig. 2D). Marked transient activation of both kinases occurred after flg22 application; activation was maximal at 5 to 10 min and then declined at 30 min, remaining only partially active at 120 min after treatment. Results revealed no differences between Col-0 and *scs9* plants with respect to the pattern of MAPK activation (Fig. 2D). All these observations, therefore, indicated that the activation of the early stage of basal immunity was not affected in the *scs9* mutant.

We next sought to demonstrate if, in a plant-DC3000 interaction, *scs9* plants might be defective in eliciting MAPK activation. Western blot analysis of protein extracts derived from Col-0, *scs9*, and *npr1* plants, the latter used as a control of a mutant, also compromised immunity and revealed positive immunoreactive signals in the two polypeptides corresponding to MPK6 and MPK3, which were visible at 24 to 48 h post-inoculation (hpi) with DC3000 (Fig. 2E). Results showed no notable differences among the three genotypes, suggesting *scs9*

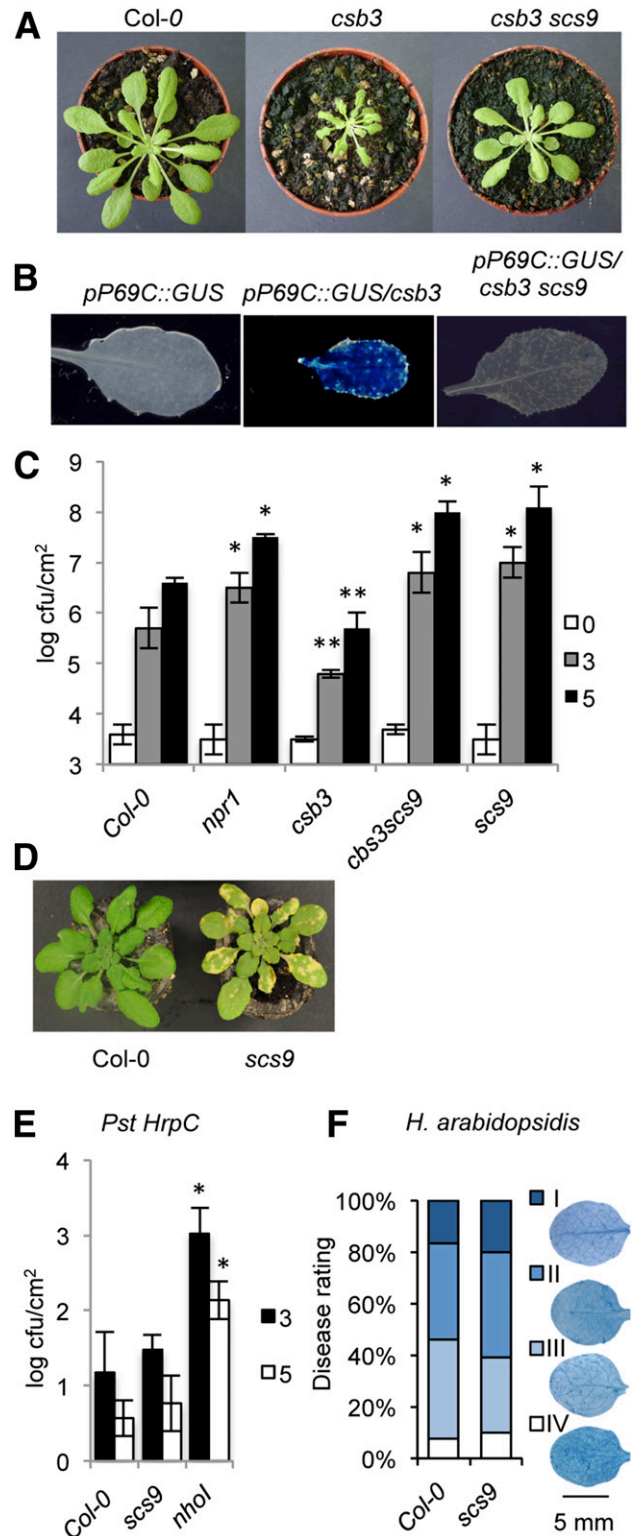
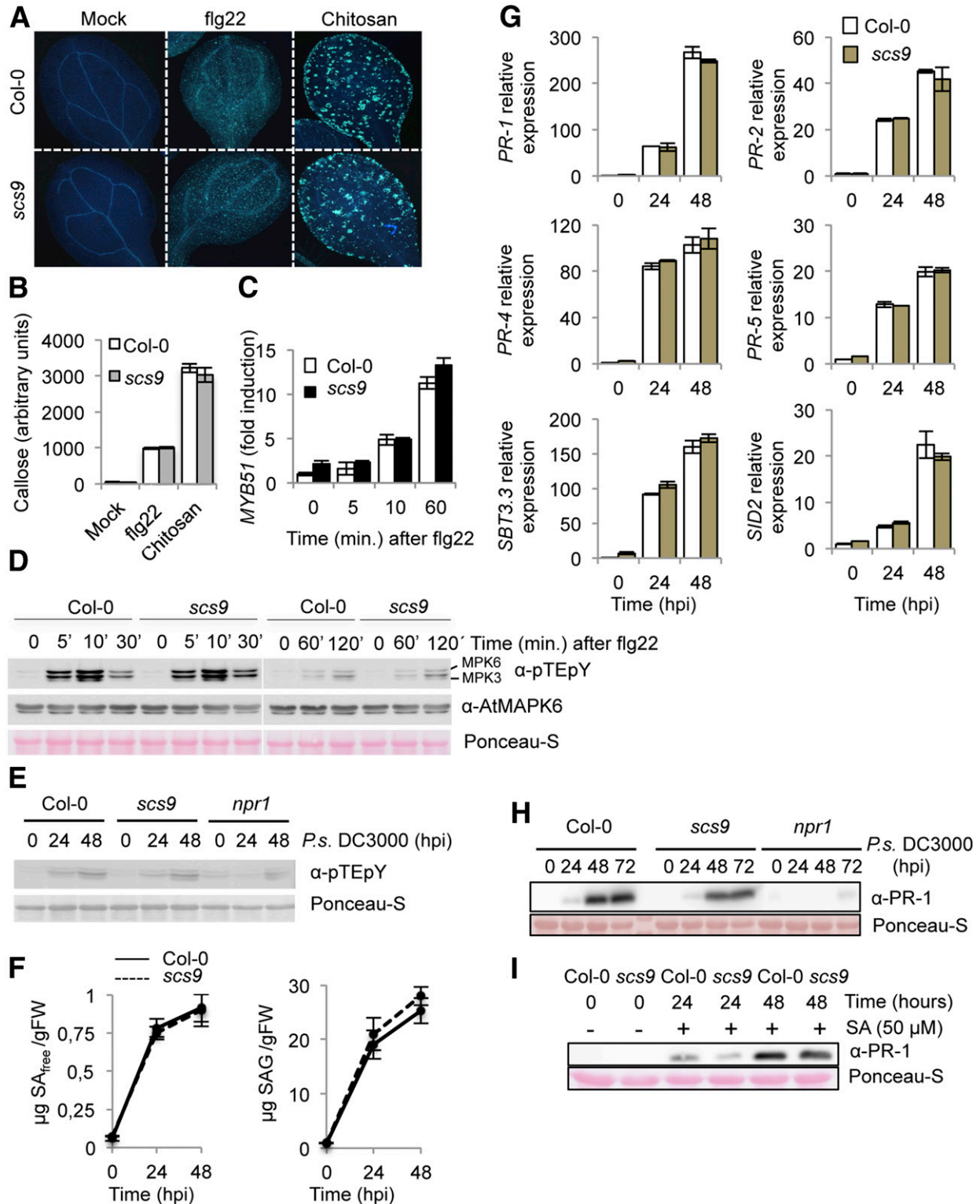


Fig. 1. Characterization of *scs9* plants. **A**, Comparison of Col-0, *csb3*, and *csb3 scs9* plants at 4 weeks after sowing. Note the stunted phenotype of the single *csb3* mutant and the growth recovery conferred by the *scs9* mutation in the double *csb3 scs9* mutant. **B**, Comparative histochemical analysis of β -glucuronidase (GUS) activity in rosette leaves from a parental wild-type Col-0 plant carrying the pP69C::GUS transgene, which shows no constitutive expression of the transgene (left), from *csb3* plants showing the constitutive activation of the transgene (center), and the reversion of this molecular phenotype in the double *csb3 scs9* mutant plant (right). **C**, Growth rates of virulent *Pseudomonas syringae* DC3000 in Col-0, *npr1-1*, *csb3*, *csb3 scs9*, and *scs9* plants. Bacterial growth was measured at zero (white bars), 3 (gray bars), and 5 (black bars) days after spray inoculation with a bacterial inoculum at an optical density at 600 nm (OD_{600}) of 0.1. Error bars represent standard deviation (SD) ($n = 12$). Asterisks indicate statistical differences to Col-0 ($P < 0.05$), using a Student's *t* test. **D**, Representatives of DC3000-inoculated Col-0 and *scs9* plants in which the *scs9* mutant exhibits a distinguishable enhancement of chlorosis due to bacterial growth. **E**, Growth rate of *Pseudomonas syringae* pv. *tomato* HrpC in Col-0, *scs9*, and *nhol* plants. Bacterial growth was measured at 3 (black bars) and 5 (white bars) days after spray inoculation with a bacterial inoculum of $OD_{600} = 0.05$. Error bars represent SD ($n = 12$). Asterisks indicate statistical differences to Col-0 ($P < 0.05$), using a Student's *t* test. **F**, Growth of *Hyaloperonospora arabidopsidis* in Col-0 and *scs9* plants. Three-week-old *Arabidopsis* seedlings were inoculated with a suspension of water containing *H. arabidopsidis* spores at a concentration of 10^5 spores per milliliter. Around 200 leaves per genotype were stained with trypan blue solution, were analyzed, and were classified in four different categories, depending on the degree of the infection (pictures panel). Class I = healthy leaves, class II = visible hyphal growth, class III = low degree of sporulation, and class IV = high degree of sporulation. The graph represents the distribution of leaves in each genotype. Differences in class distribution were statistically analyzed by a chi-square test. No statistically significant differences in the distribution of disease severity classes were observed between the two genotypes.

defects, as in *npr1*, were positioned downstream of MAPK activation following pathogen perception.

Compromised synthesis or perception of SA is on the basis explaining the compromised immunity observed in different mutants (i.e., *sid2* or *npr1*, respectively) (Cao et al. 1997; Nawrath and Métraux 1999). Consequently, we considered if *scs9* plants might carry defects in either SA biosynthesis, its accumulation, or both. Therefore, we conducted measurements to determine whether endogenous SA levels were affected in *scs9* plants. Free SA and conjugated salicylate glucoside (SAG) concentrations were comparatively examined in leaf tissues from *scs9* and Col-0 plants following DC3000 inoculation (Fig. 2F). In *scs9* plants, basal and induced amounts of free SA equaled the levels observed in Col-0 plants. SAG content was consistent with SA (Fig. 2F). This finding suggested that the increased susceptibility to DC3000 observed in *scs9* plants was not due to defects in SA biosynthesis.

We subsequently examined whether SA perception was defective in *scs9*, as detected in the *npr1* mutant, in which compromised immunity was accompanied by the absence of



induced SA-responsive gene expression (Cao et al. 1997). Therefore, induced expression of several genes diagnostic of SA-mediated disease resistance was examined by RT-qPCR in *scs9* and Col-0 plants following inoculation with DC3000. SA-responsive *PR-1*, *PR-2*, *PR-4*, *PR-5*, and *SID2* gene expression profiles, or even the recently described *SBT3.3* gene, which is pivotal in plant immunity (Ramírez et al. 2013), showed no differences in *scs9* plants when compared with Col-0 at 0, 24, and 48 hpi (Fig. 2G). This indicated transcriptional reprogramming occurred in *scs9* plants following pathogen perception. This conclusion was further supported by Western blot analysis showing that induced accumulation of PR-1 protein after bacterial infection was similar in *scs9* and Col-0 plants at 24 hpi; both genotypes showed higher accumulation of the protein at 48 and 72 hpi, with only a marginal difference in PR-1 protein accumulation observed in the mutant (Fig. 2H; Supplementary Table S2). As expected, PR-1 accumulation was nearly absent in *npr1* plants, here used as a control (Fig. 2H). These results revealed differences between *scs9* and *npr1* mutants and suggested the mutations are not allelic. Moreover, notable accumulation of PR-1 protein in response to exogenous SA application was observed in *scs9* and Col-0 (Fig. 2I); only a very slight reduction in PR-1 accumulation could be observed in *scs9* plants at 24 h after SA application further corroborating that *scs9* plants show no severe defects in SA perception.

SCS9 is At5g01230 and encodes a 2'-O-ribose tRNA MTase.

The *scs9* position was mapped by outcrossing *scs9* to Landsberg *erecta* (*Ler*) plants, and F2 plants were scored for cosegregation of enhanced susceptibility to DC3000 using simple sequence length polymorphisms (SSLPs). Thirty-five plants selected from a *Ler* × *scs9* F₂ population were analyzed and *scs9* was mapped to chromosome 5, in close proximity to the top telomeric region, and were linked to marker SGCSNP13418. We next collected 80 F2 individuals with the *scs9* phenotype and isolated individual genomes, which were bulked and deep-sequenced using the Illumina GAIIX platform. The resulting data were analyzed, using a bioinformatic pipeline devised by Austin et al. (2011), to identify a genomic region in which putative mutations of interest resided. Between the identified mapping intervals, we identified one nucleotide substitution corresponding to a G for A transition, as expected for a mutation caused by EMS mutagenesis. This resulted in a Ser for Asn substitution at position 194 of the protein encoded by the gene At5g01230 (Fig. 3A). Therefore, *SCS9* should correspond to At5g01230.

We complemented the results of our cloning strategy by searching for existing *SCS9* mutant alleles in T-DNA insertion mutant collections. One insertion mutant allele was detected, named here as *scs9-2*, which interrupted the third intron of the At5g01230 transcribed region (Fig. 3B). RT-qPCR analyses of *SCS9* transcript levels in *scs9-2* plants, compared with *scs9-1* or

Col-0 plants, revealed the absence of transcript accumulation in the former mutant (Fig. 3C). The experiment also revealed the *SCS9* gene was expressed in moderate levels in Col-0 and *scs9-1* and expression did not change following plant inoculation with DC3000 (Fig. 3C).

A comparison of disease resistance response to DC3000 between *scs9-1* and *scs9-2* plants showed both mutants were equally affected, indicating notable increased susceptibility. The heightened susceptibility was of a magnitude similar to that shown in *npr1-1* plants (Fig. 3D). The enhanced bacterial growth observed in the *scs9* mutants was very robust and reproducible. Moreover, the enhanced bacterial growth observed in the *scs9-1* and *scs9-2* mutants and in *npr1* plants was accompanied by distinguishable symptoms of induced chlorosis. This visual phenotype was not dependent on the inoculation method used, since leaf inoculation with DC3000, by infiltration with a syringe or by spraying, induced enhanced chlorosis when compared with Col-0 (Supplementary Fig. S2). Moreover, when *scs9-1* and *scs9-2* seedlings were treated with flg22 (1 μM), in a test for a microbe-associated molecular pattern–induced seedling-growth inhibition, none of the mutant alleles showed a decrease in the plant's ability to repress growth and development-related processes when compared with Col-0 (Supplementary Fig. S3). This suggests that disruption of the growth to defense shift appears not to be the reason for the observed enhanced susceptibility of *scs9* mutants to DC3000.

Next, we study the effect overexpression of *SCS9* may have on disease resistance to DC3000. *Agrobacterium*-mediated plant transformation was used to introduce into *scs9-1* (*scs9OEXSCS9* plants) and Col-0 (*wtOEXSCS9* plants) a cDNA corresponding to At5g01230, fused in-frame to green fluorescent protein (GFP) and under control of the constitutive 35S *Cauliflower mosaic virus* promoter. All 35S::*SCS9* transgenic lines generated in a *scs9-1* mutant background lost the characteristic enhanced disease susceptibility to DC3000 attributable to this mutation. Figure 3E compares bacterial growth for i) a transformed line in the *scs9-1* genetic background (i.e., line 4.4), ii) a transgenic line in the Col-0 background (i.e., line 7.4), and iii) both with respect to non-transformed *scs9-1* and Col-0 plants. *SCS9* expression restored enhanced disease susceptibility in *scs9-1* plants to Col-0 levels, further supporting the conclusion that At5g01230 is *SCS9*.

An in silico genome search for homologous amino-acid sequences revealed the highest similarity of *SCS9* was to bacterial FtsJ/RrmJ (Caldas et al. 2000), yeast Trm7p (Pintard et al. 2002), and human FTSJ1 (Bügl et al. 2000) proteins, all encoding 2'-O-ribose tRNA (MTases). Supplementary Figure S4 shows the conserved elements, including the predicted AdoMet- and the ribose-binding sites of these four tRNA MTases and the conserved amino acids that conform the catalytic tetrad (K28, D126, K166, and E201) (Pósfai et al. 1989), which is a conserved feature in 2'-O-ribose MTases exhibiting the 'MTase fold' (Bujnicki and Rychlewski 2001; Kalhor and Clarke 2003).

←

Fig. 2. Characterization of the *scs9* mutant. **A**, Callose deposition in Col-0 and *scs9* cotyledons following application of flg22 and chitosan. **B**, Callose accumulation was calculated as arbitrary units by quantifying the number of yellow pixels per million on digital micrographs of flg22- or chitosan-treated leaves at 24 h. Bars represent mean ± standard deviation (SD), *n* = 15. **C**, Time-course reverse transcription-quantitative polymerase chain reaction (RT-qPCR) analysis showing *MYB51* gene expression in Col-0 and *scs9* plants after application of flg22. Data represent mean ± SD; *n* = 3. **D**, Western blot with anti-pTEpY antibody of crude protein extracts derived from Col-0 and *scs9* plants at 0, 5, 10, 30, 60, and 120 min after treatment with flg22. Below is shown a Western blot with an anti-AtMAPK6 antibody revealing that MPK6 protein accumulated to similar levels in all the samples. Staining of the nitrocellulose filter with Ponceau-S dye confirmed an equal protein loading. The experiments were repeated three times with similar results. **E**, Western blot with anti-pTEpY antibody from Col-0, *scs9*, and *npr1-1* plants at 0, 24, and 48 h postinoculation (hpi) with *Pseudomonas syringae* DC3000. Equal protein loading was verified by staining of the nitrocellulose filter with Ponceau-S dye. The experiments were repeated three times with similar results. **F**, Free salicylic acid (SA) and conjugated salicylate glucoside (SAG) accumulation in Col-0 and *scs9* mutant at 0, 24, and 48 hpi with DC3000. Data represent the mean ± SD; *n* = 3 replicates. **G**, Time-course RT-qPCR analysis showing *PR-1*, *PR-2*, *PR-4*, *PR-5*, *SBT3.3*, and *SID2* gene expression in Col-0 and *scs9* plants after infection with DC3000. Data represent mean ± SD; *n* = 3. **H**, Western blots with anti-PR-1 antibody showing inhibition of PR-1 protein accumulation in *npr1* compared with Col-0 or in *scs9* mutant plants following inoculation with DC3000 and **I**, induced accumulation of PR-1 protein following application of SA (50 μM) in Col-0 and *scs9* plants. Experiments were repeated three times with similar results.

Arabidopsis SCS9 and the orthologous MTases from bacteria, yeast, and humans exhibited strong conservation to the predicted active site and its neighborhood, suggesting similarity to their target RNA.

Pintard et al. (2002) proposed a tRNA substrate interaction model and predicted the yeast Trm7 protein solvent-exposed side chain of S197 and R194 residues, equivalent to S199 and R196 in the *Arabidopsis* SCS9 protein, interacts specifically with the phosphate group of the methylated nucleotide. The *scs9-1* mutation is located where the conserved S194 is

substituted by N194 and lies very proximal to the mentioned residues and the catalytically important E201 tetrad residue. Therefore, it is very likely the *scs9-1* loss-of-function might be due to a lack of enzymatic activity, which would reveal the importance of the S194 residue for 2'-O-tRNA MTases.

SCS9 complements the yeast *trm7Δ* mutant.

Similarity between *Arabidopsis* SCS9 and the bona fide *S. cerevisiae* Trm7p tRNA MTase amino-acid sequences led us to investigate whether SCS9 might functionally mimic Trm7p. The deleted *S. cerevisiae* *trm7Δ* strain phenotype is characterized by slow growth compared with the wild-type strain (Pintard et al. 2002). Therefore, to examine whether the SCS9 gene provided the functions of the fission yeast TRM7 gene, we attempted complementation of a *trm7Δ* mutant strain. Unlike the vector alone (Fig. 4A), the yeast-*Escherichia coli* shuttle vector carrying the SCS9 cDNA complemented the *trm7Δ* mutant slow-growth phenotype (Fig. 4A). We therefore concluded the SCS9 gene is the *Arabidopsis* functional homolog of the TRM7 gene.

scs9 mutant is hypersensitive to paromomycin and rose bengal.

The yeast *trm7Δ* strain has been described to be highly sensitive to the antibiotic paromomycin (Pintard et al. 2002), which impairs translation by increasing codon misreading in prokaryotes and eukaryotes (Chernoff et al. 1994). Therefore, we hypothesized if SCS9 and Trm7p are functional homologs, then a *scs9* *Arabidopsis* strain might also show enhanced sensitivity to paromomycin. The *scs9-1* strain carries the kanamycin-resistance gene as a selectable marker, which might interfere with the antibiotic sensitivity assay; therefore, we employed the *scs9-2* allele that, instead, carries resistance to the herbicide BASTA as the selectable marker. Col-0 seedlings were moderately sensitive to 0.005 to 0.01% paromomycin, which partially slowed plant growth and elicited moderate anthocyanin deposition in leaves, presumably as a consequence of antibiotic imposed stress (Fig. 4B to D). Interestingly, the *scs9-2* mutant showed enhanced sensitivity to the antibiotic, as indicated from the decreased seedling growth and a concurrent increase in anthocyanin deposition in leaves of paromomycin-treated *scs9-2* plants (Fig. 4B to D). These effects were more evident at 14 μM (0.01% wt/vol) compared with 7 μM (0.005% wt/vol) antibiotic concentration, which also maximized the differences between Col-0 and *scs9-2* seedling growth. Therefore, consistent with the yeast *trm7Δ* mutant, the *Arabidopsis* *scs9-2* mutant was also highly sensitive to paromomycin.

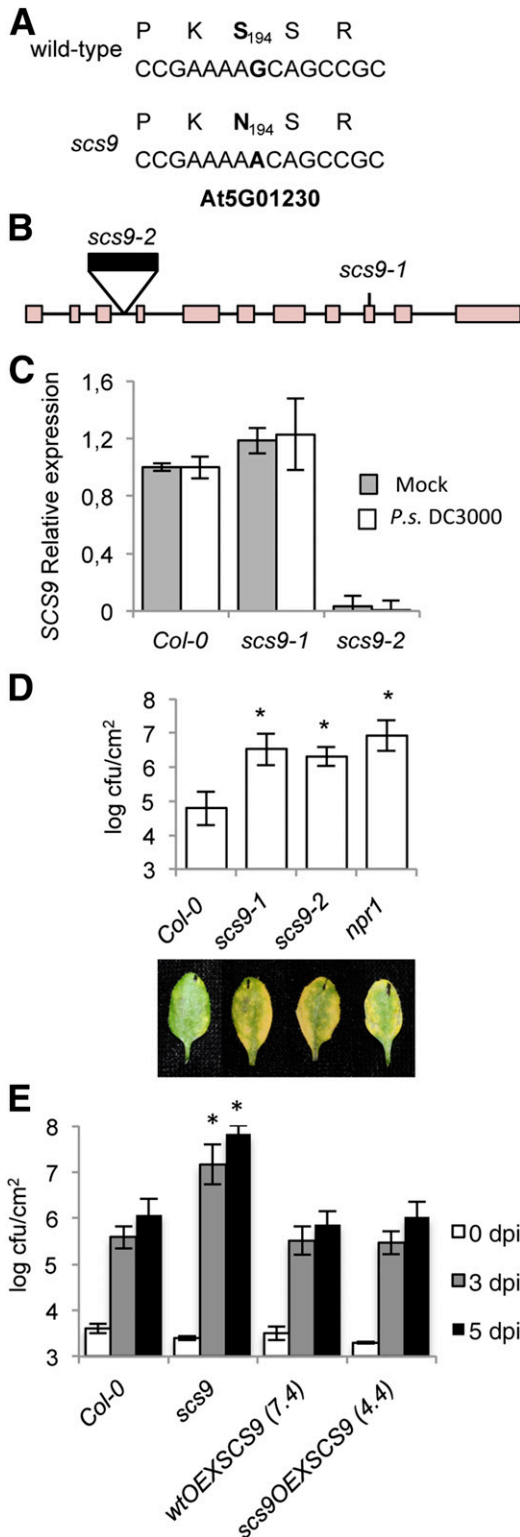


Fig. 3. *scs9* is a mutant allele of At5g01230. **A**, SCS9 corresponds to At5g01230. The G nucleotide residue mutated to an A nucleotide in the *scs9* allele is indicated in bold letters. The deduced amino-acid sequences are indicated above each nucleotide sequence, and the deduced amino-acid change (S194 to N194) is shown in bold. **B**, Intron-exon arrangement in At5g01230. Exons are shown as boxes. The distances are only approximate. Position of a T-DNA insertion in the third intron (indicated by a black box) and localization of the ethyl methanesulfonate-induced mutation in the ninth exon, rendering *scs9-2* and *scs9-1* mutant alleles, are indicated. **C**, Reverse transcription-quantitative polymerase chain reaction (RT-qPCR) analysis of the SCS9 transcript accumulation levels in mock- and *Pseudomonas syringae* DC3000-inoculated Col-0, *scs9-1*, and *scs9-2* plants at 3 days postinoculation (dpi). Data represent the mean ± standard deviation (SD), $n = 3$. **D**, Comparative growth of DC3000 in Col-0, *scs9-1*, *scs9-2*, and *npr1* plants 3 dpi. Error bars represent SD ($n = 12$). Below are representatives of inoculated leaves of the indicated genotypes. **E**, SCS9 over-expression complements the *scs9-1* mutant, and bacterial growth titers reach Col-0 levels. Plants of the indicated genotype were inoculated with DC3000. Bacterial growth was measured 0 (white bars), 3 (gray bars), and 5 (black bars) dpi. Error bars represent SD ($n = 12$). Asterisks indicate statistical differences compared with Col-0 ($P < 0.05$), analyzed using a Student's *t* test.

Moreover, Khoury et al. (2008) reported the *trm7Δ* strain was more sensitive to oxidative stress and exhibited enhanced growth inhibition in the presence of reactive oxygen species (ROS) (i.e., H₂O₂). Therefore, we examined if the *scs9* mutant became similarly more sensitive to oxidative stress. We treated *Arabidopsis* seedlings with a synthetic dye, rose bengal, which results in conditional ROS formation in the presence of light (Rózanowska et al. 1995), and we compared the responsiveness of Col-0 and *scs9-2* seedlings to this agent. Col-0 seedlings grown in petri dishes showed sensitivity after 5 days of exposure to 2 μM rose bengal, which elicited partial chlorosis in leaves, reduction in root growth, and inhibition of lateral root formation (Fig. 4E). *scs9-2* mutant seedlings exhibited increased sensitivity to the dye, which became bleached instead of chlorotic, and seedlings eventually died after 5 days of exposure (Fig. 4E). Therefore, both yeast *trm7Δ* and *Arabidopsis scs9* mutants displayed hypersensitive responses to this type of ROS-derived stress condition. In contrast, *scs9-1*, *scs9-2*, and Col-0 seedlings are equally sensitive to salt-derived stress, as recorded in seedling growth inhibition and germination assays performed with increasing concentrations (i.e., 0, 50, 100, and 200 mM) of NaCl (Supplementary Fig. S5). These differences might indicate a selectivity for this specific tRNA 2'-*O*-ribose MTase in mediating adaptation to specific stressing situations.

SCS9 localizes to the nuclei, including the nucleolus.

Although tRNA molecules are transcribed in the nucleus, they can function in different subcellular compartments, emphasizing the importance of an appropriate distribution and localization of tRNA modifying enzymes. Moreover, mature tRNA move from the cytoplasm to the nucleus via retrograde tRNA nuclear import, a process proposed to function as a pathway that monitors end processing of pre-tRNAs (Kramer and Hopper 2013). Our objective was to identify the cellular compartment in which SCS9 exerted its function as a potential tRNA modifier. We therefore used a SCS9 tagged to green fluorescent protein (GFP) or mCherry protein, which was functional in complementing the *scs9* phenotype (Fig. 3E), and performed colocalization studies using confocal microscopy. The free GFP or specific subnuclear compartment marker proteins were used upon transient agroinfiltration of *Nicotiana benthamiana* leaves with *Agrobacterium* strains carrying each corresponding gene construct. eIF4A, a RNA helicase component of the exon junction complex (eIF4A-mRFP) and the histone H3 variant cenH3 (CENH3-mRFP) colocalized with SCS9-mCherry in the nucleolus and nucleoplasm (Fig. 5; panels iv and v), indicating SCS9 partial enrichment or preference for the nucleolus. Coilin (Coilin-mRFP) and U2b'' (U2b''-GFP), two Cajal body markers and other nuclear bodies

often associated with the nucleolus, also confirmed SCS9 localization in the nucleus and its preference for the nucleolus but not for any type of nuclear bodies (Fig. 5; panels ii and iii). Finally, free GFP, which accumulated in the cytoplasm and nucleus but was excluded from the nucleolus, allowed a clear identification of SCS9-mCherry in the nucleolus (Fig. 5; panel i). Therefore, we concluded that SCS9 is preferentially localized in the nucleus and exhibited preference for the nucleolus. These results suggested modifications of tRNA molecules,

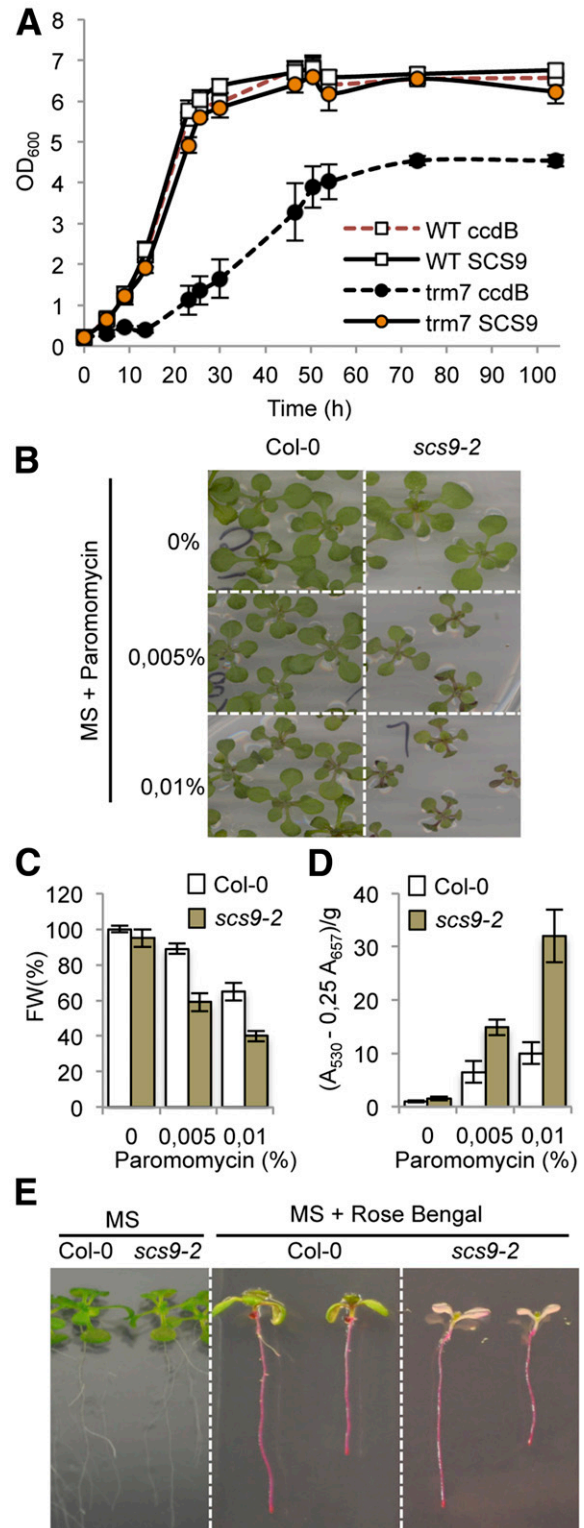


Fig. 4. Complementation of the *Saccharomyces cerevisiae trm7Δ* strain with *Arabidopsis SCS9* cDNA and hypersensitivity of *scs9-2* seedlings to paromomycin and rose bengal. **A**, Comparative growth curves of various *S. cerevisiae* strains grown in yeast potato dextrose at 30°C. Open squares represent wild-type strains (BMA64) transformed with plasmid p423-GAL1 alone (WT ccdB) or using a plasmid carrying an *Arabidopsis SCS9* cDNA (WT SCS9). Filled circles represent the *trm7Δ* strain transformed with the plasmid alone (*trm7 ccdB*), or with the plasmid carrying the *Arabidopsis SCS9* cDNA (*trm7 SCS9*). **B**, Col-0 and *scs9-2* seedling growth in mass spectrometry (MS) plates alone or in the presence of 0.005% (wt/wt) and 0.01% (wt/wt) of paromomycin. **C**, Quantitative analysis of paromomycin effects on growth retardation in Col-0 and *scs9-2* seedlings measured as reduction in fresh weight (FW). **D**, Quantitative analysis of anthocyanins accumulation in Col-0 and *scs9-2* seedlings treated with paromomycin at the indicated concentrations. **E**, Differential effects of rose bengal on growth inhibition of Col-0 and *scs9-2* seedlings grown in MS plates.

directed by the MTase enzyme, most likely occur in the nucleus and not the cytoplasm.

SCS9 is required for tRNA 2'-O-ribose methylation in vivo.

Based on the close structural similarities between SCS9 and Trm7p, FtsJ/RrmJ, and FTSJ MTases, we tested whether SCS9 was similarly involved in 2'-O-ribose methylation of nucleotides in the *Arabidopsis* tRNAs anticodon loop. Positions 32 and 34 in the anticodon loop (Fig. 6A) were identified as concurrent targets of Trm7p-like MTases (Pintard et al. 2002). Modified nucleotides corresponding to *Arabidopsis* tRNAs potentially altered due to defects in SCS9 were identified by comparing Col-0 modifications with those that commonly differed in *scs9-1* and *scs9-2* mutants. We used young seedlings as a source of plant material, which, according to our previous experiences, show higher abundance of RNA. tRNA isolation, degradation, and subsequent high-pressure liquid chromatography (HPLC) analysis of separated nucleosides were

performed as previously described (Chen et al. 2010); elution time, and spectrum of each peak were used to identify different modified nucleosides. Characteristic chromatograms of Col-0, *scs9-1*, and *scs9-2* plants are shown in Supplementary Figure S6. Twenty-one major modified nucleosides were detected in the three genetic backgrounds, which all fit into previously identified modifications in *Arabidopsis* (Chen et al. 2010). Notably, HPLC chromatogram comparison between Col-0 and the two mutants revealed *scs9-1* and *scs9-2* plants carried identical conspicuous diminutions in 2'-O-methylated cytidine (Cm) content when compared with other invariant modified nucleosides such as 7-methyl guanosine (m⁷G) or 1-methyl guanosine (m¹G). Cm-modified nucleosides showed 70% reduction in *scs9-1* and *scs9-2* plants compared with Col-0 plants (Fig. 6B). In addition, 2'-O-methylated uridine (Um) content showed a 30% reduction in both mutants (Fig. 6B). However, in *scs9-1* and *scs9-2* mutants, the decrease in 2'-O-methylated guanosine (Gm) was consistently much less, at only 10 to 15% reduction (Fig. 6B). More accurate and straightforward determination of 2'-O-methylated cytosine (Cm) content by liquid chromatography-mass spectrometry (LC-MS) confirmed the notable reduction observed by HPLC analysis in *scs9-1* and *scs9-2* plants when compared with Col-0 plants (Fig. 6C). Interestingly, following DC3000 inoculation, Col-0 plants showed a moderate but progressive accumulation of Cm with a statistically significant 60% enhancement occurring at 72 and 120 h.p.i when compared with its control at 0 hpi (Fig. 6C). Conversely, *scs9-1* and *scs9-2* plants were impaired in this pathogen-mediated enhancement of Cm (Fig. 6C). For Um nucleoside modification (Fig. 6C), and to a lesser extent also for Gm (Supplementary Fig. S7), LC-MS quantification revealed similar enhanced accumulation in Col-0 at 72 to 120 hpi. These enhancements were not observed to occur in *scs9-1* and *scs9-2* plants (Fig. 6C).

The three nucleoside modifications are highly conserved modifications in the tRNA anticodon loop, Cm occurring at positions 32 and 34, Um at position 32, and Gm at position 34 (Fig. 6A). Positions 32 and 34 are known targets of Trm7p-like MTase, it is therefore likely that SCS9 is similarly required for 2'-O-ribose methylation at position 32 and 34. In yeast, Wilkinson et al. reported cytosine and uracil nucleotides at position 4 of tRNAs (Fig. 6A) were also 2'-O-methylated (Wilkinson et al. 2007); however at this position ribose methylation was Trm7p-independent, and instead required the Trm13p methyltransferase. It remains unknown whether Um and Cm at position 4 occurs in plants, and if a Trm13-like enzyme regulates these specific modifications.

The 2'-O-ribose modifications at positions 32 and 34 of the anticodon loop revealed by our study occurred in tRNA^{Phe(GmAA)}, tRNA^{Trp(CmCA)} and tRNA^{Leu(UmAA)} (El Yacoubi et al. 2012; Pintard et al. 2002). Reduced 2'-O-methylated nucleoside accumulation observed in *scs9-1* and *scs9-2* mutants might result from reduced accumulation of the respective tRNA precursors. We therefore performed Northern blots of small RNAs extracted from Col-0 and the two *scs9* mutants, and hybridized the filters with radiolabeled probes specific for each of the three indicated tRNAs. The nonrelated tRNA^{Gln} was used as an internal control. Noticeable changes in RNA accumulation were not observed in any genetic backgrounds for any tRNAs examined (Fig. 6D). In addition, alterations in tRNA content were not detected following DC3000 inoculation. However, at this stage we cannot disregard the possibility that other functional aspects of tRNA metabolism, like those related to the relative level of charged and uncharged tRNAs may become altered in the *scs9* mutants.

Therefore, the marked reduction in Cm and Um accumulation, and to a minor extent in Gm, common to the *scs9* mutants,

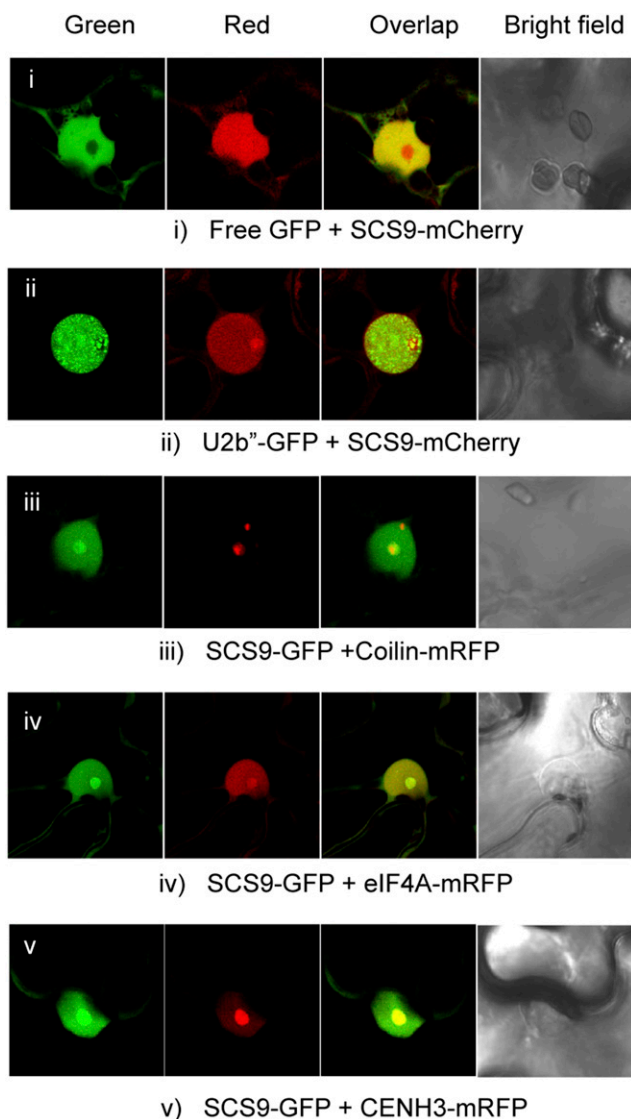


Fig. 5. SCS9 nuclear localization. Colocalization patterns of SCS9, fused to either green fluorescent protein (GFP) or mCherry, with free GFP (panel i) and several different nuclear tagged proteins, including U2b'' (panel ii), Coilin (panel iii), eIF4A (panel iv), and CENH3 (panel v) in epidermal cells from *Nicotiana benthamiana* transfected with each respective pair of constructs, evaluated by confocal microscopy.

is a consequence of 2'-*O*-methyl transferase loss-of-function, and which appeared to have no effect on transcript levels of corresponding tRNAs.

DISCUSSION

In the present report, we employed a variety of approaches to define a relationship between specific tRNA modifications at the anticodon loop, and the execution of an effective immune response toward DC3000 in *Arabidopsis*. Identification of the *scs9* mutant, which suppressed the previously described *csb3*-associated enhanced disease resistance phenotype, indicated that SCS9 was pivotal for plant resistance toward this pathogen. Moreover, the observation that *scs9* plants allow a similar growth of the biotrophic pathogen *H. arabidopsidis* indicates that SCS9 is required to mount an effective resistance specifically against *P. s.* DC3000. In addition, *scs9* shows a wild-type-like response to this pathogen when its Type III secretion system is removed, suggesting that the enhanced susceptibility of *scs9* plants to DC3000 is dependent on bacterial effectors and thus related to effector-triggered immunity (ETI). In *scs9* plants the molecular hallmarks associated with activation of immune responses were properly activated; however, despite these measures *scs9* plants were unable to fend off DC3000. Therefore *scs9* plants possess a critical distinction that differentiates *scs9* from other mutant plants with a similar compromised immunity. NPR1 is the central regulator of SA-mediated plant immunity toward DC3000 (Yan and Dong 2014), and therefore the *npr1* mutant is unable to resist DC3000 infections. However, at variance with the *npr1* mutant, *scs9* plants are not compromised in SA perception and neither on its accumulation. This makes a clear distinction between *npr1* and *scs9* plants, suggesting that the defect(s) in *scs9* plant resistance operate downstream or distant to the point of *npr1* failed control.

Map-based cloning and sequence analysis revealed SCS9 is homologous to yeast Trm7p (Pintard et al. 2002), human FTSJ1 protein (Bügl et al. 2000), and bacterial FtsJ/RrmJ proteins (Caldas et al. 2000), encoding 2'-*O*-ribose tRNA MTases. These enzymes exhibited the common "MTase fold" (Bujnicki and Rychlewski 2001), suggesting their biological target tRNA must be similar. In fact, SCS9 provided the fission yeast Trm7p functions, demonstrated by effective complementation of a *trm7Δ* mutant using *Arabidopsis* SCS9 cDNA, and providing unequivocal evidence the SCS9 gene is the *Arabidopsis* functional homolog of the *TRM7* gene. The mechanistic relationship between Trm7p and SCS9 was further established by the observation that loss of either protein makes corresponding *trm7Δ* and *scs9* mutant cells sensitive to oxidative stress and also sensitive to paromomycin, an antibiotic that impairs translation by increasing codon misreading (Chernoff et al. 1994). However, this enhanced sensitivity of the *scs9* mutants is not manifested when other type of abiotic stress, such as saline stress, is imposed. These results thus give support to the importance of this specific tRNA 2'-*O*-ribose MTase for plants to selectively cope with only certain types of stress and adds to the growing body of evidences indicating that other tRNA nucleoside modification genes are pivotal to cope with imposed stress conditions (Burgess et al. 2015; David et al. 2017; Huang and Hopper 2016; Wang et al. 2017; Zhou et al. 2013). Moreover, consistent with *trm7Δ*, *Arabidopsis* *scs9* plants were defective in the 2'-*O*-ribose methylation of nucleotides 32 and 34 of the tRNAs anticodon loop. The marked reduction in Cm content and, to a lesser degree, in Um and Gm at nucleotides 32 and 34, all of them targets of yeast Trm7p MTase (Pintard et al. 2002), reinforced our conclusion that *Arabidopsis* SCS9 and yeast Trm7p MTases are homologous. Furthermore, the observation

that Cm content and, to a similar extent, also Um content enhance upon infection of Col-0 plants with DC3000 and that their deficiency correlates with a defective immune response gives relevance to SCS9 as a new component regulating effectiveness of plant resistance against DC3000. Our observation on the importance of tRNA modification in biotic stress response thus adds to the observation of Pajerowska-Mukhtar et al. (2012), who reported that the levels of uncharged tRNA corresponding to phenylalanine were shown to rapidly and transiently increase in response to pathogen attack to allow translation of TBF1, a key defense regulator important to mediated SA-mediated immunity (Xu et al. 2017a). Even though this latter study focused on a different regulatory step of translation in plant immunity, the evidences also points toward the importance of tRNA metabolism as a point of control regulating biotic stress adaptation.

Then, how can a defect in Cm at specific tRNA wobble positions interfere with plant resistance while maintaining an intact upstream signal transduction pathway normally required for mounting an efficient plant immune response? We speculate that, following DC3000 inoculation, reprogramming of specific tRNA wobble modifications led to selective translation of mitochondrial RNA (mRNA) species enriched with the cognate codon, in a manner similar to that described in other eukaryotes (Chan et al. 2010; Wang and He 2014). The absence of accurate modifications at the wobble position in specific tRNAs would drive inefficient translation or generate misreading of specific proteins, which would be vital for an effector-triggered immune response. This translational control is congruent with SCS9 operating downstream of NPR1 and of its subordinated transcriptional reprogramming during the defense response. Moreover, these observations represent an additional layer of complexity in the control of the global translational reprogramming that occurs during induction of resistance in plants (Xu et al. 2017b) and gives further support to the existence of mechanisms in which tRNA-derived nucleoside modifications control translation of proteins under stress (Chan et al. 2012; Dedon and Begley 2014; Gu et al. 2014). However, it is important to note *scs9* mutants carried no gross alterations at the protein synthesis and accumulation levels, as deduced from the normal protein pattern observed in sodium dodecyl sulfate (SDS) polyacrylamide gels or from the normal accumulation of host-induced pathogenesis-related proteins (e.g., PR-1) interpreted from Western blot analysis. This favors a hypothesis in which defects derived from *scs9* mutations would very likely elicit impacts at the proteome level in a very specific manner, presumably affecting only translation in a selective group of proteins with a pivotal role for effective execution of the immune response program. The literature provides some evidence for specific tRNA modification-dependent translation control during stress response in higher eukaryotes and, particularly, to oxidative stress. For example, Kalhor and Clarke (2003) showed that yeast Trm9 catalyzed methyl esterification leads to conversion of uracil into mcm⁵U at the wobble position of tRNA^{Arg}(U^{CU}) and tRNA^{Glu}(U^{UC}). This process enhanced binding of the anticodon and, therefore, facilitated translation of AGA- and GAA-rich transcripts, which functionally maps to processes of stress signaling to fend off deleterious effects of ionic radiation on DNA damage (Begley et al. 2007). Similarly, Trm4, which catalyzes m⁵C at the wobble position of tRNA^{Leu}(C^{AA}), enhanced translation efficiency of mRNAs enriched in the UUG codon recognized by this tRNA, and loss of Trm4 caused hypersensitivity to the cytotoxic effects of H₂O₂ (Jackman et al. 2003), a phenotype also observed to occur in the *trm4b* mutant defective in a tRNA MTase that renders 5-methylcytosine (m⁵C) (David et al. 2017). One of these UUG-biased mRNAs whose translation is controlled

Our results also led us to hypothesize that the absence of specific methylation at the wobble position of the selective group of tRNAs controlled by SCS9 might affect the synthesis of one or more codon-biased cognate proteins required for resistance to DC3000, which might function as repressor proteins. If the repressor is defective or poorly translated, then a cellular factor or molecular process might become depressed, which in turn might favor bacterial growth and host colonization. This may reconcile with the existence of tRNA cleaving toxins, developed by certain microbes to act on specific positions within the anticodon loop of target tRNAs, such as colicin and onconase (Phizicky and Hopper 2010) or the γ -toxin of *Kluyveromyces lactis* that targets and cleaves specific tRNAs in the yeast *S. cerevisiae* that have the mcm⁵s²U modification at position 34 of tRNA^{Glu(UUU)} (Lu et al. 2005). At this stage, we cannot disregard the idea that bacterial effector proteins may have been developed to target specific modified plant tRNAs or even the MTase responsible for such tRNA modification as part of a pathogenic strategy.

We cannot ignore the possibility of a surveillance mechanism leading to hypomodified tRNA degradation as part of a conserved response to stress (Kadaba et al. 2004; Motorin and Helm 2010), which might have a potential impact on translation and disease progression, as described by Thompson and Parker (2009). The emergence of tRNA-derived fragments as a novel class of small regulatory RNAs (Lee et al. 2009; Pederson 2010) with potential roles as regulators of gene silencing and genome stability, through the targeting of transposable element transcripts (Maute et al. 2013; Raina and Ibba 2014; Schorn et al. 2017), and, as part of a conserved stress response also described in plants (Martinez et al. 2017; Thompson et al. 2008), might therefore interfere with epigenetic processes governed by small RNAs, such as RNA-directed DNA methylation, which has recently been demonstrated as pivotal for plant immunity to DC3000 (López et al. 2011). However, this latter mechanism seems less likely, since the hypomodified tRNA levels in *scs9* plants appeared not to be degraded, not even following inoculation with the pathogen.

In summary, the present results denote the importance of keeping intact tRNA modifications for mounting an effective disease resistance response toward DC3000. Unraveling further components, its regulation, and identifying target proteins whose translation is regulated by these tRNAs modifications will open new avenues to better understand how the effectiveness of disease resistance is regulated in plants.

MATERIALS AND METHODS

Plant growth conditions.

Arabidopsis thaliana plants were grown in a growth chamber (19 to 23°C) on a 10-h light and 14-h dark cycle as previously

described (Ramírez et al. 2013). All mutants are in Col-0 background.

β -Glucuronidase (GUS) staining and callose deposition analysis.

Protocols for GUS staining and determination of callose deposition in plant leaves were performed as previously described (Coego et al. 2005; García-Andrade et al. 2013).

Mapping and cloning.

The *scs9* mutant was backcrossed twice to the *csb3* line to confirm its recessive inheritance; *scs9* plants were crossed to *Ler*; and F1 plants were allowed to self. F2 plants were scored for cosegregation of enhanced disease susceptibility to DC3000 with SSLPs (Bell and Ecker 1994; López et al. 2011). Molecular markers were derived from the polymorphism database between the *Ler* and Col-0 ecotypes (The *Arabidopsis* Information Resource website). Whole-genome sequencing and identification of nucleotide polymorphisms was carried out at the John Innes Centre (Norwich, U.K.) as a genome service exchange, using an Illumina GAIIx platform and the bioinformatic pipeline devised by Austin et al. (2011).

Gene constructs and expression in yeast and transgenic plants.

To amplify *SCS9* cDNA, PCR was performed using the Expand high-fidelity PCR system (Roche), with 1 μ l of cDNA, using *BPSCS9Fw* and *BPSCS9Rv* specific primers including Gateway adapters and recombined to *pDONR221* using Gateway technology (Life Technologies) and were recombined into the different destination vectors using LR ClonaseMixII kit (Invitrogen). For the *SCS9-GFP* overexpressing construct, *pDONR221 SCS9* was recombined to *pB7FWG* destination. For the *SCS9-mCherry* overexpressing construct, *pDONR221 SCS9* was recombined to the modified *pEarlyGate101* vector (García-Andrade et al. 2013). For the yeast *trm7* complementation assay, *pDONR221 SCS9* vector was recombined to the yeast expression vectors *p423-GAL1* and *p423-GAL1-GFP*, to generate *p423 GAL1/SCS9* and *p423 GAL1/SCS9-GFP*, respectively. Individual clones were sequenced to confirm absence of errors in the *SCS9* cDNA. *p423 GAL1/SCS9*, *p423 GAL1/SCS9-GFP*, and the respective empty vectors were transformed into wild type (*BMA64*, *MAT α* [Pintard et al. 2002]) and *trm7p* (*YBL4409*, *MAT α* , *trm7 Δ :TRP1* [Pintard et al. 2002]) yeast strains as previously described (Castelló et al. 2011) and were grown on agar plates lacking His. Transformants were then transferred to selective liquid media containing 2% (wt/vol) Gal to induce expression of *SCS9*. These cultures were incubated at 28°C for 2 days, and then, were adjusted to an optical density at 600 nm (OD₆₀₀) = 0.1 to perform the time-course growing assays.

Fig. 6. Reduced content of transfer RNA (tRNA)-derived 2'-O-methylcytosine (Cm), 2'-O-methyluracil (Um), and 2'-O-methylguanine (Gm) in *scs9-1* and *scs9-2* mutants. **A**, Position of common modifications found in cytoplasmic tRNA in *Arabidopsis* and its major domains. tRNA is shown in its common secondary structure form, with circles representing nucleotides and lines representing base pairs. Positions in shaded gray indicate the proposed tRNA methylation site for Trm7-like MTases in eukaryotes. Residue 34 corresponds to the wobble nucleotide. AAS = amino acid-accepting stem, DSL = dihydrouridine stem and loop, ASL = anticodon stem loop, and VL = variable loop. Conventional abbreviations for nucleotide modifications are used (the Modomics database). **B**, Percent reduction of Cm, Um, and Gm content in *scs9-1* and *scs9-2* relative to Col-0 plants as determined by high-pressure liquid chromatography analysis. Each value was relative to the amount of tRNA-derived 7-methylguanosine (m⁷G) and 1-methylguanosine (m¹G), which remained invariant in all the genotypes. Data points represent the average of three biological replicates. **C**, Relative content of Cm- and Um-modified nucleosides in Col-0, *scs9-1*, and *scs9-2* plants during the course of an infection with *Pseudomonas syringae* DC3000, as determined by liquid chromatography-mass spectrometry. Samples were taken at 0, 24, 48, 72, and 120 h postinoculation (hpi). Each value was relative to the amount of tRNA-derived m¹G, which remained invariant during the infection process. Data represent the mean \pm standard deviation; $n = 3$. Asterisks indicate statistical differences compared with its respective genotype as referred to its time 0 control ($P < 0.05$), analyzed using a Student's *t* test. **D**, tRNA Northern blot in mock- and DC3000-inoculated Col-0, *scs9-1*, and *scs9-2* plants. Leaf samples were collected at 3 days postinoculation. The membranes were hybridized with radiolabel probes to tRNA^{Phe}, tRNA^{Gln}, tRNA^{Leu}, tRNA^{Trp}. Equal RNA loading was verified by staining with EtBr (bottom panel).

Transient expression in *Nicotiana benthamiana* leaves and confocal laser-scanning microscopy.

Fully expanded leaves of *N. benthamiana* were agro-infiltrated with a suspension of *Agrobacterium tumefaciens* C58 bearing the relevant construct, and this plant tissue was analyzed with a Leica TCS LS spectral confocal microscope as previously described (Dobón et al. 2015).

RT-qPCR.

qPCR assays were performed, using an ABI PRISM 7000 sequence detection system and SYBR Green (Perkin-Elmer Applied Biosystems), as described previously (García-Andrade et al. 2013). *ACTIN2* was used as a reference gene.

Western blots.

Protein crude extracts, SDS-polyacrylamide gel electrophoresis, and immunoblots were performed as previously described (Dobón et al. 2015).

***Pseudomonas syringae* inoculations.**

Arabidopsis leaves were inoculated with DC3000 as previously described (Coego et al. 2005; Gil et al. 2005; López et al. 2011; Ramírez et al. 2010, 2013), using a bacterial inoculum at a final OD₆₀₀ of 0.1, with 0.02% Silwet L-77 (Crompton Europe) if inoculated by spray or with a further 1:500 dilution (without Silwet L-77) when inoculation was performed by leaf infiltration with a syringe.

***H. arabidopsidis* assays.**

H. arabidopsidis WACO9 was cultivated in susceptible *NahG* plants in Wassileskij background. The spores were collected by washing the sporulating tissue with autoclaved water and were subsequently cleaned by filtering using two Miracloth layers. The inoculum was prepared by measuring and adjusting the spore concentration using a Neubauer chamber. For the mutant analysis, 3-week-old *Arabidopsis* seedlings were inoculated with a suspension of water containing *H. arabidopsidis* spores at a concentration of 10⁵ spores per milliliter and were kept in high humidity conditions. Six days after spraying, around 200 infected leaves per genotype, from a population of around 50 seedlings, were lactophenol trypan blue-stained (100 mg of trypan blue, 50 mg of phenol, 50 mg of glycerol 100%, 50 ml of lactic acid, water to 150 ml volume, plus 300 ml of Ethanol Absolute), and were preserved in 60% chloral hydrate. The disease progression was scored by direct visualization of the samples using a stereomicroscope. Infected leaves were assigned to four different categories based on the degree of infection: class I = healthy leaves, class II = discrete pathogen growth and no sporulation, class III = high degree of pathogen growth and reduce sporulation (from 1 to 5 spores), and class IV = high degree of pathogen growth and sporulation.

T-DNA *Arabidopsis* mutants.

T-DNA insertion mutants and primers used to identify insertions by PCR are listed in Supplementary Table S3.

tRNA isolation, digestion, HPLC, and LC-MS analysis.

Total RNA was extracted using Trizol reagent (Invitrogen), small RNAs were separated from ribosomal RNA and mRNA using LiCl, and tRNA was further purified using cellulose DE52 resin (Whatman) as described by Chen et al. (2010). tRNA (100 µg) dissolved in Milli-Q water was degraded to nucleosides with P1 nuclease (Sigma Aldrich) and alkaline phosphatase (Toyobo), as described by Chen et al. (2010). The modified nucleosides were analyzed using Reverse-phase HPLC (Waters Alliance HPLC system and Waters Absorbance Detector 2996) and a C-30 column (Develosil C-30

reverse-phase column, 250 × 4.6 mm; Nomura Chemical Co., Ltd.). The buffer gradient was as described (Chen et al. 2010). Modified nucleosides were quantified relative to two internal standards (m⁷G and m¹G). For LC-MS analysis, total RNA and microRNA was extracted using a microRNA extraction kit (Omega Bio-Tek Inc.). RNA concentration was determined using a NanoDrop ND-1000 spectrophotometer (Thermo Scientific), about 20 µg tRNA was digested with 2 U P1 nuclease (Sigma) and 1.5 U of calf-intestine alkaline phosphatase (Toyobo) in 20 µl of 20 mM HEPES-KOH (pH 7.0) at 37°C for 3 h. Sample was diluted with MilliQ water (Millipore Synergy) to a concentration of 5 µg/ml, the injected volume was 10 µl. API 4000 Q-TRAP mass spectrometer (Applied Biosystems) was used with an LC-20A HPLC system and a diode array UV detector (190 to 400 nm) equipped with an electro spray ionization source. Electrospray ionization MS was conducted in a positive ion mode. The nebulizer gas, auxiliary gas, curtain gas, turbo gas temperature, entrance potential, and ion spray voltage were 60 psi, 65 psi, 15 psi, 550°C, 10 V, and 5,500 V, respectively. Multiple reaction monitoring mode was performed to determine parent-to-product ion transitions. An Inertsil ODS-3 (2.1 mm × 150 mm, 5 µm particle size; Shimadzu) reversed-phase column with an Inertsil ODS guard column (4 mm × 10 mm, 5 µm particle size; Shimadzu) was used for chromatographic separation of nucleosides. The mobile phase gradient consisted of 2 mM ammonium acetate (solvent A) and methanol (solvent B). The flow rate was 0.6 ml/min at ambient temperature. Nucleoside standard uridine, cytidine, adenosine, guanosine, 1-methyladenosine, 7-methylguanosine, 5-methyluridine and 2'-*O*-methylguanosine nucleoside standards (Santa Cruz Biotechnology) were used to distinguish nucleoside isomers. The relative abundance of each selected modified nucleoside was calculated as area of the peak with the correct mass and parent-to-product ion transition divided by total area for uridine, cytidine, adenosine, and guanosine monitored nucleosides. Then, the relative content of Cm, Um, and Gm nucleosides was related to one or both m¹G and m⁷G.

Anthocyanin and SA quantification.

Anthocyanin extraction and quantification was performed as previously described (Ramírez et al. 2010). SA extraction and quantification was performed as described (Defraia et al. 2008; Huang et al. 2005).

Paromomycin and rose bengal assays.

Seeds were sterilized and stratified in darkness at 4°C for 3 days and were transferred to growth chambers for each assay. To conduct paromomycin rate assay, seeds were plated on Murashige and Skoog medium (Duchefa Biochemie) supplemented with 0.5% sucrose, without or with paromomycin. Pictures were taken after 14 days. To conduct the rose bengal assay, seeds sown on Murashige and Skoog plates were vertically grown for 4 days under normal conditions, and then, seedlings were transferred to vertical square MS plates with or without 2 µM rose bengal. The pictures were taken after 7 days.

tRNA blot analysis.

Total RNA was extracted from leaf tissue using TRIzol (Invitrogen), following the manufacturer's protocol. A total of 4 µg of RNA was electrophoresed 15% (wt/vol) polyacrylamide gels under denaturing conditions and was then transferred to Hybond N (Amersham) membranes. Oligonucleotide probes were 32P-labeled with T4 polynucleotide kinase (Fermentas), according to manufacturer's instructions, and were then purified on a microspin G-25 column, separating labeled probe from unincorporated nucleotides. The specific activity was

determined using scintillation counter. Prehybridization of the membranes was carried out for 30 min in Church hybridization buffer (0.5 M NaPO₄ [pH 7.2], 7% [wt/vol] SDS). Hybridization was carried out in the same buffer overnight at 40°C, followed by three washes at the same temperature for 20 min each in 0.5× SSC/0.1% SDS (1× SSC is 0.15 M NaCl plus 0.015 M sodium citrate) (Church and Gilbert 1984).

Flg22 treatments and NaCl growth assay.

For flg22 treatment, seedlings were grown and treated with 1 μM flg22 as previously described (García-Andrade et al. 2011). For saline growth assay and effect on germination, sterilized seeds were plated on Murashige and Skoog solid supplemented with 0.5% sucrose and morpholineethanesulfonic acid (MES) (0.01%), without or with NaCl (at different concentrations). Pictures and fresh weight data were taken after 13 days. To analyze seedling growth inhibition by salt stress, seeds sown and grown under normal conditions (without NaCl) for 6 days were transferred to Murashige and Skoog medium without and with NaCl (at different concentrations). Pictures and data of fresh weight were taken after 7 days of treatment; 20 seedlings were analyzed for each replicate. For seedling growth-inhibition assays by flg22, 7-day-old seedlings, grown in Murashige and Skoog solid plates (with 0.5% sucrose and 0.01% MES), were transferred to Murashige and Skoog liquid media, with or without 1 μM flg22, and were softly shaken (90 rpm) for 5 days, and the fresh weight from groups of 10 seedling of each genotype was measured.

ACKNOWLEDGMENTS

We acknowledge B. Lapeyre for providing *S. cerevisiae* *trm7Δ* mutant strain and plasmids, G. Etherington and B. Wulff for assistance in genome sequencing of *scs9* mutant, P. Tornero for the *Pseudomonas syringae*, *HrpC*, and *Acinetobacter* strains and assistance in SA determination, L. Pérez for her assistance on the identification of the initial *csb3 scs9* mutant.

LITERATURE CITED

Agris, P. F., Vendeix, F. A., and Graham, W. D. 2007. tRNA's wobble decoding of the genome: 40 years of modification. *J. Mol. Biol.* 366:1-13.

Asai, T., Tena, G., Plotnikova, J., Willmann, M. R., Chiu, W. L., Gomez-Gomez, L., Boller, T., Ausubel, F. M., and Sheen, J. 2002. MAP kinase signalling cascade in Arabidopsis innate immunity. *Nature* 415:977-983.

Austin, R. S., Vidaurre, D., Stamatou, G., Breit, R., Provart, N. J., Bonetta, D., Zhang, J., Fung, P., Gong, Y., Wang, P. W., McCourt, P., and Guttman, D. S. 2011. Next-generation mapping of Arabidopsis genes. *Plant J.* 67:715-725.

Begley, U., Dyavaiah, M., Patil, A., Rooney, J. P., DiRenzo, D., Young, C. M., Conklin, D. S., Zitomer, R. S., and Begley, T. J. 2007. Trm9-catalyzed tRNA modifications link translation to the DNA damage response. *Mol. Cell* 28:860-870.

Bell, C. J., and Ecker, J. R. 1994. Assignment of 30 microsatellite loci to the linkage map of *Arabidopsis*. *Genomics* 19:137-144.

Bethke, G., Unthan, T., Uhrig, J. F., Pöschl, Y., Gust, A. A., Scheel, D., and Lee, J. 2009. Flg22 regulates the release of an ethylene response factor substrate from MAP kinase 6 in *Arabidopsis thaliana* via ethylene signaling. *Proc. Natl. Acad. Sci. U.S.A.* 106:8067-8072.

Björk, G. R. 1995. Biosynthesis and function of modified nucleosides. Pages 165-205 in: *tRNA: Structure, Biosynthesis and Function*. D. Soll and U. L. RajBhandary, ed. American Society for Microbiology, Washington, D.C.

Bügl, H., Fauman, E. B., Staker, B. L., Zheng, F., Kushner, S. R., Saper, M. A., Bardwell, J. C., and Jakob, U. 2000. RNA methylation under heat shock control. *Mol. Cell* 6:349-360.

Bujnicki, J. M. and Rychlewski, L. 2001. Reassignment of specificities of two cap methyltransferase domains in the reovirus lambda 2 protein. *Genome Biol.* 2:research0038.1.

Burgess, A., David, R., and Searle, I. R. 2016. Deciphering the epitranscriptome: A green perspective. *J. Integr. Plant Biol.* 58:822-835.

Burgess, A. L., David, R., and Searle, I. R. 2015. Conservation of tRNA and rRNA 5-methylcytosine in the kingdom Plantae. *BMC Plant Biol.* 15:199.

Caldas, T., Binet, E., Bouloc, P., Costa, A., Desgres, J., and Richarme, G. 2000. The FtsJ/RrmJ heat shock protein of *Escherichia coli* is a 23 S ribosomal RNA methyltransferase. *J. Biol. Chem.* 275:16414-16419.

Cao, H., Glazebrook, J., Clarke, J. D., Volko, S., and Dong, X. 1997. The Arabidopsis *NPR1* gene that controls systemic acquired resistance encodes a novel protein containing ankyrin repeats. *Cell* 88:57-63.

Castelló, M. J., Carrasco, J. L., Navarrete-Gómez, M., Daniel, J., Granot, D., and Vera, P. 2011. A plant small polypeptide is a novel component of DNA-binding protein phosphatase 1-mediated resistance to *Plum pox virus* in Arabidopsis. *Plant Physiol.* 157:2206-2215.

Chan, C. T., Dyavaiah, M., DeMott, M. S., Taghizadeh, K., Dedon, P. C., and Begley, T. J. 2010. A quantitative systems approach reveals dynamic control of tRNA modifications during cellular stress. *PLoS Genet.* 6:e1001247.

Chan, C. T., Pang, Y. L., Deng, W., Babu, I. R., Dyavaiah, M., Begley, T. J., and Dedon, P. C. 2012. Reprogramming of tRNA modifications controls the oxidative stress response by codon-biased translation of proteins. *Nat. Commun.* 3:937.

Chen, P., Jäger, G., and Zheng, B. 2010. Transfer RNA modifications and genes for modifying enzymes in *Arabidopsis thaliana*. *BMC Plant Biol.* 10:201.

Chernoff, Y. O., Vincent, A., and Liebman, S. W. 1994. Mutations in eukaryotic 18S ribosomal RNA affect translational fidelity and resistance to aminoglycoside antibiotics. *EMBO J.* 13:906-913.

Church, G. M., and Gilbert, W. 1984. Genomic sequencing. *Proc. Natl. Acad. Sci. U.S.A.* 81:1991-1995.

Clay, N. K., Adio, A. M., Denoux, C., Jander, G., and Ausubel, F. M. 2009. Glucosinolate metabolites required for an *Arabidopsis* innate immune response. *Science* 323:95-101.

Coego, A., Ramirez, V., Ellul, P., Mayda, E., and Vera, P. 2005. The H₂O₂-regulated *Ep5C* gene encodes a peroxidase required for bacterial speck susceptibility in tomato. *Plant J.* 42:283-293.

David, R., Burgess, A., Parker, B., Li, J., Pulsford, K., Sibbritt, T., Preiss, T., and Searle, I. R. 2017. Transcriptome-wide mapping of RNA 5-methylcytosine in Arabidopsis mRNAs and noncoding RNAs. *Plant Cell* 29:445-460.

Dedon, P. C., and Begley, T. J. 2014. A system of RNA modifications and biased codon use controls cellular stress response at the level of translation. *Chem. Res. Toxicol.* 27:330-337.

Defraia, C. T., Schmelz, E. A., and Mou, Z. 2008. A rapid biosensor-based method for quantification of free and glucose-conjugated salicylic acid. *Plant Methods* 4:28.

Deng, W.-L., Preston, G., Collmer, A., Chang, C.-J., and Huang, H.-C. 1998. Characterization of the *hrpC* and *hrpRS* operons of *Pseudomonas syringae* pathovars *syringae*, *tomato*, and *glycinea* and analysis of the ability of *hrpF*, *hrpG*, *hrpC*, *hrpT*, and *hrpV* mutants to elicit the hypersensitive response and disease in plants. *J. Bacteriol.* 180:4523-4531.

Dobón, A., Canet, J. V., García-Andrade, J., Angulo, C., Neumetzler, L., Persson, S., and Vera, P. 2015. Novel disease susceptibility factors for fungal necrotrophic pathogens in Arabidopsis. *PLoS Pathog.* 11:e1004800.

El Yacoubi, B., Bailly, M., and de Crécy-Lagard, V. 2012. Biosynthesis and function of posttranscriptional modifications of transfer RNAs. *Annu. Rev. Genet.* 46:69-95.

García-Andrade, J., Ramirez, V., Flors, V., and Vera, P. 2011. Arabidopsis *ocp3* mutant reveals a mechanism linking ABA and JA to pathogen-induced callose deposition. *Plant J.* 67:783-794.

García-Andrade, J., Ramirez, V., López, A., and Vera, P. 2013. Mediated plastid RNA editing in plant immunity. *PLoS Pathog.* 9:e1003713.

Gil, M. J., Coego, A., Mauch-Mani, B., Jordá, L., and Vera, P. 2005. The *Arabidopsis* *csb3* mutant reveals a regulatory link between salicylic acid-mediated disease resistance and the methyl-erythritol 4-phosphate pathway. *Plant J.* 44:155-166.

Gu, C., Begley, T. J., and Dedon, P. C. 2014. tRNA modifications regulate translation during cellular stress. *FEBS Lett.* 588:4287-4296.

Guy, M. P., Podyma, B. M., Preston, M. A., Shaheen, H. H., Krivos, K. L., Limbach, P. A., Hopper, A. K., and Phizicky, E. M. 2012. Yeast Trm7 interacts with distinct proteins for critical modifications of the tRNA^{Phe} anticodon loop. *RNA* 18:1921-1933.

Hori, H. 2014. Methylated nucleosides in tRNA and tRNA methyltransferases. *Front. Genet.* 5:144.

Huang, H.-Y., and Hopper, A. K. 2016. Multiple layers of stress-induced regulation in tRNA biology. *Life (Basel)* 6:16.

Huang, W. E., Wang, H., Zheng, H., Huang, L., Singer, A. C., Thompson, I., and Whiteley, A. S. 2005. Chromosomally located gene fusions constructed in *Acinetobacter* sp. ADP1 for the detection of salicylate. *Environ. Microbiol.* 7:1339-1348.

Jackman, J. E., Montange, R. K., Malik, H. S., and Phizicky, E. M. 2003. Identification of the yeast gene encoding the tRNA^mG methyltransferase responsible for modification at position 9. *RNA* 9:574-585.

- Jordá, L., and Vera, P. 2000. Local and systemic induction of two defense-related subtilisin-like protease promoters in transgenic Arabidopsis plants. *Luciferin induction of PR gene expression. Plant Physiol.* 124: 1049-1058.
- Jühling, F., Mörl, M., Hartmann, R. K., Sprinzl, M., Stadler, P. F., and Pütz, J. 2009. tRNADB 2009: compilation of tRNA sequences and tRNA genes. *Nucleic Acids Res.* 37:D159-D162.
- Kadaba, S., Krueger, A., Trice, T., Krecic, A. M., Hinnebusch, A. G., and Anderson, J. 2004. Nuclear surveillance and degradation of hypomodified initiator tRNA^{Met} in *S. cerevisiae*. *Genes Dev.* 18:1227-1240.
- Kalhor, H. R., and Clarke, S. 2003. Novel methyltransferase for modified uridine residues at the wobble position of tRNA. *Mol. Cell. Biol.* 23: 9283-9292.
- Khoury, C. M., Yang, Z., Li, X. Y., Vignali, M., Fields, S., and Greenwood, M. T. 2008. A TSC22-like motif defines a novel antiapoptotic protein family. *FEMS Yeast Res.* 8:540-563.
- Kirchner, S., and Ignatova, Z. 2015. Emerging roles of tRNA in adaptive translation, signalling dynamics and disease. *Nat. Rev. Genet.* 16: 98-112.
- Kramer, E. B., and Hopper, A. K. 2013. Retrograde transfer RNA nuclear import provides a new level of tRNA quality control in *Saccharomyces cerevisiae*. *Proc. Natl. Acad. Sci. U.S.A.* 110:21042-21047.
- Kuchino, Y., Borek, E., Grunberger, D., Mushinski, J. F., and Nishimura, S. 1982. Changes of post-transcriptional modification of wye base in tumor-specific tRNA^{Phe}. *Nucleic Acids Res.* 10:6421-6432.
- Lee, Y. S., Shibata, Y., Malhotra, A., and Dutta, A. 2009. A novel class of small RNAs: tRNA-derived RNA fragments (tRFs). *Genes Dev.* 23: 2639-2649.
- López, A., Ramírez, V., García-Andrade, J., Flors, V., and Vera, P. 2011. The RNA silencing enzyme RNA polymerase v is required for plant immunity. *PLoS Genet.* 7:e1002434.
- Lu, J., Huang, B., Esberg, A., Johansson, M. J., and Byström, A. S. 2005. The *Kluyveromyces lactis* γ -toxin targets tRNA anticodons. *RNA* 11: 1648-1654.
- Machnicka, M. A., Milanowska, K., Osman Oglou, O., Purta, E., Kurkowska, M., Olchowik, A., Januszewski, W., Kalinowski, S., Dunin-Horkawicz, S., Rother, K. M., Helm, M., Bujnicki, J. M., and Grosjean, H. 2013. MODOMICS: a database of RNA modification pathways—2013 update. *Nucleic Acids Res.* 41:D262-D267.
- Machnicka, M. A., Olchowik, A., Grosjean, H., and Bujnicki, J. M. 2014. Distribution and frequencies of post-transcriptional modifications in tRNAs. *RNA Biol.* 11:1619-1629.
- Martinez, G., Choudury, S. G., and Slotkin, R. K. 2017. tRNA-derived small RNAs target transposable element transcripts. *Nucleic Acids Res.* 45: 5142-5152.
- Mauro, V. P., and Edelman, G. M. 2007. The ribosome filter redux. *Cell Cycle* 6:2246-2251.
- Maute, R. L., Schneider, C., Sumazin, P., Holmes, A., Califano, A., Basso, K., and Dalla-Favera, R. 2013. tRNA-derived microRNA modulates proliferation and the DNA damage response and is down-regulated in B cell lymphoma. *Proc. Natl. Acad. Sci. U.S.A.* 110:1404-1409.
- Miyawaki, K., Tarkowski, P., Matsumoto-Kitano, M., Kato, T., Sato, S., Tarkowska, D., Tabata, S., Sandberg, G., and Kakimoto, T. 2006. Roles of Arabidopsis ATP/ADP isopentenyltransferases and tRNA isopentenyltransferases in cytokinin biosynthesis. *Proc. Natl. Acad. Sci. U.S.A.* 103:16598-16603.
- Motorin, Y., and Helm, M. 2010. tRNA stabilization by modified nucleotides. *Biochemistry* 49:4934-4944.
- Nawrath, C., and Métraux, J. P. 1999. Salicylic acid induction-deficient mutants of Arabidopsis express PR-2 and PR-5 and accumulate high levels of camalexin after pathogen inoculation. *Plant Cell* 11:1393-1404.
- Novoa, E. M., Pavon-Eternod, M., Pan, T., and Ribas de Pouplana, L. 2012. A role for tRNA modifications in genome structure and codon usage. *Cell* 149:202-213.
- Pajerowska-Mukhtar, K. M., Wang, W., Tada, Y., Oka, N., Tucker, C. L., Fonseca, J. P., and Dong, X. 2012. The HSF-like transcription factor TBF1 is a major molecular switch for plant growth-to-defense transition. *Curr. Biol.* 22:103-112.
- Pederson, T. 2010. Regulatory RNAs derived from transfer RNA? *RNA* 16: 1865-1869.
- Phizicky, E. M., and Hopper, A. K. 2010. tRNA biology charges to the front. *Genes Dev.* 24:1832-1860.
- Pintard, L., Lecoq, F., Bujnicki, J. M., Bonnerot, C., Grosjean, H., and Lapeyre, B. 2002. Trm7p catalyses the formation of two 2'-O-methylriboses in yeast tRNA anticodon loop. *EMBO J.* 21:1811-1820.
- Pósfai, J., Bhagwat, A. S., Pósfai, G., and Roberts, R. J. 1989. Predictive motifs derived from cytosine methyltransferases. *Nucleic Acids Res.* 17: 2421-2435.
- Raina, M., and Ibba, M. 2014. tRNAs as regulators of biological processes. *Front. Genet.* 5:171.
- Ramírez, V., López, A., Mauch-Mani, B., Gil, M. J., and Vera, P. 2013. An extracellular subtilase switch for immune priming in Arabidopsis. *PLoS Pathog.* 9:e1003445.
- Ramírez, V., Van der Ent, S., García-Andrade, J., Coego, A., Pieterse, C. M., and Vera, P. 2010. OCP3 is an important modulator of NPR1-mediated jasmonic acid-dependent induced defenses in Arabidopsis. *BMC Plant Biol.* 10:199.
- Różanowska, M., Ciszewska, J., Korytowski, W., and Sarna, T. 1995. Rose-bengal-photosensitized formation of hydrogen peroxide and hydroxyl radicals. *J. Photochem. Photobiol. B* 29:71-77.
- Schorn, A. J., Gutbrod, M. J., LeBlanc, C., and Martienssen, R. 2017. LTR-retrotransposon control by tRNA-derived small RNAs. *Cell* 170:P61-71. E11.
- Takano, K., Nakagawa, E., Inoue, K., Kamada, F., Kure, S., and Goto, Y.; Japanese Mental Retardation Consortium. 2008. A loss-of-function mutation in the FTSJ1 gene causes nonsyndromic X-linked mental retardation in a Japanese family. *Am. J. Med. Genet. B. Neuropsychiatr. Genet.* 147B:479-484.
- Thompson, D. M., Lu, C., Green, P. J., and Parker, R. 2008. tRNA cleavage is a conserved response to oxidative stress in eukaryotes. *RNA* 14: 2095-2103.
- Thompson, D. M., and Parker, R. 2009. Stressing out over tRNA cleavage. *Cell* 138:215-219.
- Walden, T. L., Jr., Howes, N., and Farkas, W. R. 1982. Purification and properties of guanine, queuine-tRNA transglycosylase from wheat germ. *J. Biol. Chem.* 257:13218-13222.
- Wang, X., and He, C. 2014. Dynamic RNA modifications in post-transcriptional regulation. *Mol. Cell* 56:5-12.
- Wang, Y., Li, D., Gao, J., Li, X., Zhang, R., Jin, X., Hu, Z., Zheng, B., Persson, S., and Chen, P. 2017. The 2'-O-methyladenosine nucleoside modification gene OsTRM13 positively regulates salt stress tolerance in rice. *J. Exp. Bot.* 68:1479-1491.
- Wilkinson, M. L., Crary, S. M., Jackman, J. E., Grayhack, E. J., and Phizicky, E. M. 2007. The 2'-O-methyltransferase responsible for modification of yeast tRNA at position 4. *RNA* 13:404-413.
- Xu, G., Greene, G. H., Yoo, H., Liu, L., Marqués, J., Motley, J., and Dong, X. 2017a. Global translational reprogramming is a fundamental layer of immune regulation in plants. *Nature* 545:487-490.
- Xu, G., Yuan, M., Ai, C., Liu, L., Zhuang, E., Karapetyan, S., Wang, S., and Dong, X. 2017b. uORF-mediated translation allows engineered plant disease resistance without fitness costs. *Nature* 545:491-494.
- Yan, S., and Dong, X. 2014. Perception of the plant immune signal salicylic acid. *Curr. Opin. Plant Biol.* 20:64-68.
- Yewdell, J. W., Antón, L. C., and Binnink, J. R. 1996. Defective ribosomal products (DRiPs): A major source of antigenic peptides for MHC class I molecules? *J. Immunol.* 157:1823-1826.
- Zhou, W., Karcher, D., and Bock, R. 2013. Importance of adenosine-to-inosine editing adjacent to the anticodon in an Arabidopsis alanine tRNA under environmental stress. *Nucleic Acids Res.* 41:3362-3372.

AUTHOR-RECOMMENDED INTERNET RESOURCES

- The Arabidopsis Information Resource website:
<https://www.arabidopsis.org>
 The MODOMICS database: <http://modomics.genesilico.pl>